

# Unsteady Kutta Condition at High Values of the Reduced Frequency Parameter

F.S. Archibald\*

University of Cambridge, Cambridge, England

The unsteady Kutta condition is discussed in the light of some recent experimental measurements made near the trailing edge of a long flat plate and a 10C4 airfoil. The hierarchy of disagreement from the theoretically predicted zero trailing edge loading caused by viscous instabilities is found to be acoustically correlated vortex shedding, natural vortex shedding, Tollmien-Schlichting waves, and, by implication, turbulent boundary-layer eddies. The region of significant chordwise disagreement scales with the wake perturbation wavelength of the corresponding instability. Coordinating the vorticity of the turbulent boundary layer shed from the profile airfoil with a transverse acoustic resonance produced a distinct disagreement of the Kutta condition at high reduced frequency parameters ( $\lambda = wc/U$ ). In this case and for vortex shedding, the extrapolated loading coefficient at the trailing edge increased with the nondimensional acoustic amplitude.

## I. Introduction

THE Kutta condition as applied in unsteady potential airfoil analyses is essentially an extension of steady theory. Kutta<sup>1</sup> postulated that a value of circulation should be chosen in his steady potential model to avoid a velocity singularity at the sharp trailing edge of an airfoil. This condition can be established if the trailing edge is also the rear stagnation point. The resulting modeled flow pattern agrees with that observed in steady flow and also predicts the lift and its chordwise distribution well at low angles of attack. The theoretical consequences of this hypothesis are that the lift loading or chordwise vorticity jump approaches zero at the trailing edge. An alternative statement is that the surface velocities on either side of the airfoil approach a common value at the rear stagnation point.

For rounded trailing edges, the position of the rear stagnation point is indeterminate, as there is no velocity singularity to be avoided and so fix its location. In this case and for the situation of real flows with viscosity, Taylor<sup>2</sup> proposed the condition of zero net vorticity discharge to establish the steady lift value. Preston<sup>3</sup> explained the deviation of the lift of an airfoil at low angles of incidence from the potential theory value as due to the profile alteration from the boundary-layer growth. His calculations incorporated Taylor's vorticity discharge condition. Various approximate steady lift calculation methods for the rounded trailing edge geometry have been proposed by Gostello<sup>4</sup> and others. These extend the upper and lower lift distributions, at a selected chordwise position, to the trailing edge to give zero loading and thereby remove the stagnation point indeterminacy.

In the unsteady case there are all the previous theoretical difficulties and, in addition, the unsteady effects on the viscous boundary layer and the shed vorticity. The latter complicates the airfoil response, making it a function of the airfoil's vorticity history. However, same theoretical assumption for the Kutta condition, of no unsteady loading at the

Received September 30, 1974; revision received November 25, 1974. The research referred to in this paper was performed at the University of Cambridge Engineering Department and comprises the body of the author's thesis. Thanks are accorded the members of staff, technicians and especially the author's supervisor, D.S. Whitehead, who suggested and guided the investigation. Grateful acknowledgement is also made to the Ministries of Technology and Defense who supported the work.

Index categories: Boundary-Layer Stability and Transition; Non-steady Aerodynamics.

\* Graduate student, Engineering Department; presently Acoustic Engineer, Pratt & Whitney Aircraft, East Hartford, Conn.

trailing edge, is made in linearized analyses for isolated airfoils and those in cascades or wind tunnels.

Experimental incompressible work with oscillating airfoils in wind tunnels has revealed that as the reduced frequency parameter increases, the complex lift increasingly deviates from linear theory both in magnitude and phase. The most recent and extensive tests were done by Greidanus, van der Vooren, and Bergh.<sup>5</sup> They extended the range of the reduced frequency parameter, ( $\lambda = wc/U$ ) to 2.0 for an airfoil mechanically oscillated separately in heaving and pitching modes. They observed and corrected the boundary-layer transition point motion with a trip wire. The experimental disagreement from the Theodorsen<sup>6</sup> potential theory was ascribed to the Kutta condition not holding since other errors introduced were considered too small to account for the discrepancy.

Fujita and Kovasznay<sup>7</sup> report on the response of a stationary instrumented airfoil to the wake from an upstream rotating rod. This unsteady flow situation has importance in turbomachinery aerodynamic analyses, and Fourier decomposition of the sharp edged gust implies very high frequency parameters. The measured chordwise response was in good agreement with linear theory over most of the chord except for the final 10%. In this region theoretical agreement is poor due to loading at the trailing edge.

Compressible unsteady airfoil theory in cascade with direct applicability to the acoustic resonance case, discussed later, is that of Wollaston and Runyan.<sup>8</sup> Their work on the effect of the wind tunnel walls on the unsteady lift preceded the acoustic resonance classification by Parker<sup>9</sup> for the cascade configuration. They studied the usual experimental wind tunnel situation of small chord to pitch ratio. This would have given Parker resonances little different from the first cross-mode of the tunnel. They calculated the effect this resonance would have on the unsteady aerodynamic coefficient measurements, and suggested that wind tunnel tests should be designed to avoid this resonance. Whitehead<sup>10</sup> in a linearized compressible cascade analysis calculated the effect on the lift of an oscillated blade when its motion excited the Parker  $\beta$ -mode. In both these numerical calculations the Kutta condition was assumed.

At intermediate values of the reduced frequency parameter for airfoils in cascade, Smith<sup>11</sup> calculated the sound generated by passage of unloaded rotor blades through a stationary sinusoidal velocity field. Since he achieved very good experimental agreement acoustically, there is inferential evidence that the unsteady response of the cascade agrees with linear compressible theory at low Mach number when there is no steady lift on the blades.

It is noted that the percentage of the total lift is not great

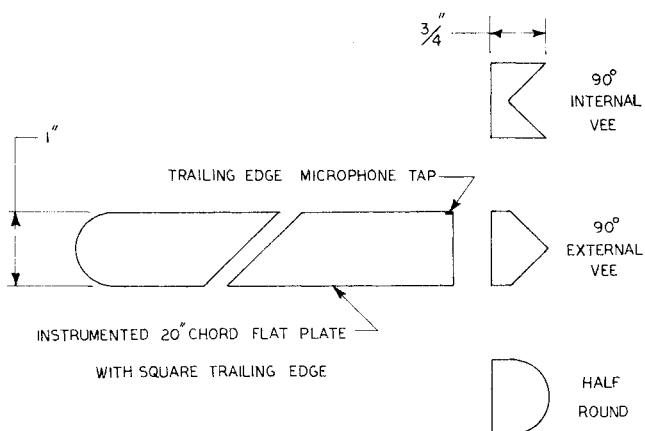


Fig. 1 Different geometries attached to the square trailing edge flat plate.

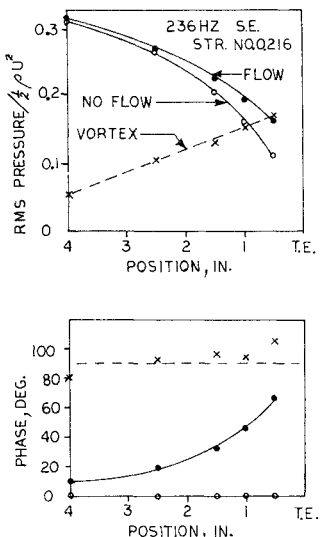


Fig. 2 The chordwise pressure distribution on the 20 in. flat plate during self-excitation showing the  $\beta$  mode and vortex components.

near the trailing edge and a large local discrepancy might not change the total lift by much. However, measurements made in this region can be used to correct existing steady and unsteady linear analyses.

Tanner<sup>12</sup> reports that the slope of the steady lift coefficient for a NACA 65A006 airfoil is 10% greater with a modified blunt ended rear portion than the correct profile. Clearly the flow instability of vortex shedding acts favorably on the unsteady airfoil lift performance. Although, as will be shown, the unsteady field does not satisfy the Kutta condition, this instability does not prevent the steady flow from doing so. This result suggests that treating the steady and unsteady flows separately is valid and that the effects can be superpositioned without significant interaction.

There has also been work on the unsteady Kutta condition as applied at the lip of a nozzle. In this case, there is a steady vorticity jump at the nozzle edge. Although there have been suggested a few theoretical modifications to the Kutta condition by Orszag and Crow,<sup>13</sup> experiments by Becker and Pfizenmaier<sup>14</sup> find that there is no velocity singularity at the nozzle lip when the flow is acoustically perturbed.

Recently the author has published articles<sup>15,16</sup> which have included measurements of the unsteady pressures near the trailing edges of an airfoil and a bluff plate. The main thrust of those publications was with regard to the mechanics and manner of self-excitation of an acoustic resonance by two different trailing edge flow instabilities. Here those results will be examined with regard to existing unsteady airfoil analyses. The resonance was also used to simulate the heaving motion

of an airfoil which made possible an investigation of the unsteady Kutta condition at high  $\lambda$  values when the boundary layer was turbulent.

## II. Discussion of Results

The experimental results to be discussed were obtained using a specially designed test section of a low speed wind tunnel. There were two full span airfoils at zero incidence involved in the study of the self-excitation of the Parker  $\beta$ -mode resonance. This antisymmetric transverse acoustic resonance, the design of the test section, and the instrumented airfoils used are described more fully in Refs. 15 and 16. Both airfoils had a  $1/2$  in. Brüel and Kjaer microphone installed with a series of selectable pressure taps in the trailing edge region (20% of the chord). The 20 in. flat plate had an unsteady pressure tap in the base and the steady base pressure was measured using three holes at mid-span connected to a common plenum. The base pressure measurements were only done for the square trailing edge. Figure 1 shows the various trailing edge shapes that were attached to the basic square ended flat plate. The 10C4 airfoil only had provision for measuring the unsteady surface pressures.

The most severe violation of the unsteady Kutta condition is the case of acoustically correlated vortex shedding. Figure 2 from Ref. 15 shows the chordwise surface pressure distribution in the trailing edge region during self-excitation of the acoustic resonance for the square trailing edge geometry. At each chordwise station the acoustic resonance pressure was subtracted vectorially from the combined pressures when self-exciting to obtain the purely incompressible vortex shedding pressure.

During self-excitation the acoustic field is present in sufficient amplitude to "lock" the vortex shedding frequency to the acoustic frequency, and the shedding is correlated across the span. For this case there is a total spanwise violation of the Kutta condition and the loading at the trailing edge is twice the surface pressure of one side. The linear chordwise loading distribution for acoustically locked vortex shedding extends the same distance upstream (approximately one wake perturbation wavelength from the trailing edge) independent of Strouhal number.

The amplitude of the trailing edge loading increased with the amplitude of the locking acoustic field. This is defined in

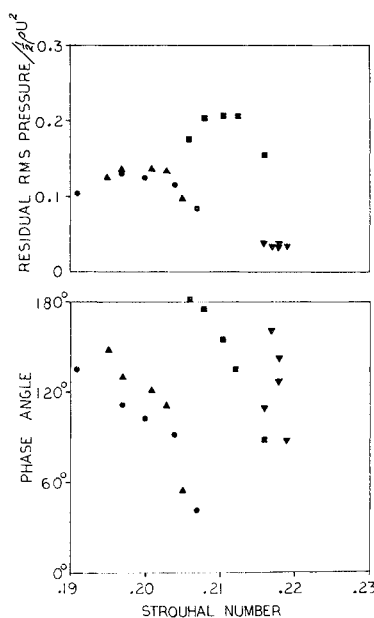


Fig. 3 The residual Strouhal response of the square ■, round ●, convex ▲, and concave ▼ geometry  $3/4$  in. from the trailing edge of the 1 in. flat plate.

Table 1 Residual root mean square lift coefficients for acoustically correlated vortex shedding

Trailing edge geometry	Str. no for $P_{0\max}^*$	Maximum residual pressure coef- ficients $\frac{1}{2}\rho U^2$ from trailing edge	$P_{0\max}^*$ phase	Integrated trailing edge lift coefficient
Concave right angle	0.218	0.040	145°	0.235
Square at end	0.210	0.240	135°	1.20
Square ( $\frac{1}{4}$ in. from end)	0.210	0.205	135°	1.20
Convex right angle	0.199	0.135	125°	0.79
Half round	0.197	0.130	112°	0.765
Cylinder Ref. 17	0.180	...	112°	0.30

Ref. 15 as the feedback gain in the self-exciting system. In addition, the amplitude and phase of the vortex shedding had a Strouhal number response similar to a damped single-degree-of-freedom oscillator, although the phase of the vortex shedding pressure to the acoustic mode decreased as the Strouhal number increased. This is characteristic of a negatively damped system and is associated with the energy released by this instability phenomena. Figure 3 shows the residual response behavior for the different trailing edges. The residual designation (\*) means the purely incompressible pressure which exists for correlated vortex shedding with no acoustic field present. The curve was obtained by extrapolating the vortex pressure measurements at the trailing edge during self-excitation (Fig. 8, Ref. 15) to zero acoustic amplitude using the acoustic feedback gain. It is seen that as the trailing edge geometry goes from convex to concave the Strouhal number for the maximum value of the pressure coefficient increases, as does the corresponding phase.

Table 1 compares the maximum values of the residual surface pressure coefficient  $P_{0\max}^*/\frac{1}{2}\rho U^2$  for the various trailing edge shapes. The rear most tap in the instrumented flat plate was  $\frac{3}{4}$  in. from the actual trailing edge for all shapes except the square. Due to the antisymmetry of the locking acoustic mode, the local pressure loading is twice these values. An estimate of the integrated lift coefficient  $C_{l\max}^*$  in the trailing edge region is shown in the last column. The same extent and linear distribution as measured for the square trailing edge was used for each trailing edge geometry. These integrated acoustically correlated residual-lift values are compared with the maximum lift value reported by Tanaka and Takahara<sup>17</sup> for a circular cylinder mechanically oscillated with an amplitude 3.3% of the diameter. The coefficients are of similar magnitude indicating that the full effect of the wake has been reflected onto the effectively semi-infinite flat plate near the trailing edge. The cylinder has a low diameter to wake wavelength ratio and thus is totally within the near field of the wake instability.

The acoustic mode was used as the phase reference for the trailing edge results. Since the resonance velocities occur in quadrature, the mode pressure has the same phase relation as the displacement for the cylinder. The lift and Strouhal number for the cylinder in Table 1 were chosen for the same phase as the round trailing edge.

Figure 4a shows the increase of the steady base drag associated with the increase of the acoustic amplitude. This was first reported by Wood<sup>18</sup> and is shown below to be the result of the increase in the locked vortex shedding caused by the acoustic field. The single curve was obtained using data from three resonances of the perturbation apparatus for the square trailing edge geometry. No direct comparison is possible between the three cases because the Strouhal number was not held constant and the mode shapes, although transverse, were not identical. However, Fig. 4b shows a similar slope for the increase of the trailing edge surface pressure with the same nondimensional acoustic amplitude. As this latter curve represents the magnitude of the unsteady vorticity shed into the wake, it suggests that the increase in

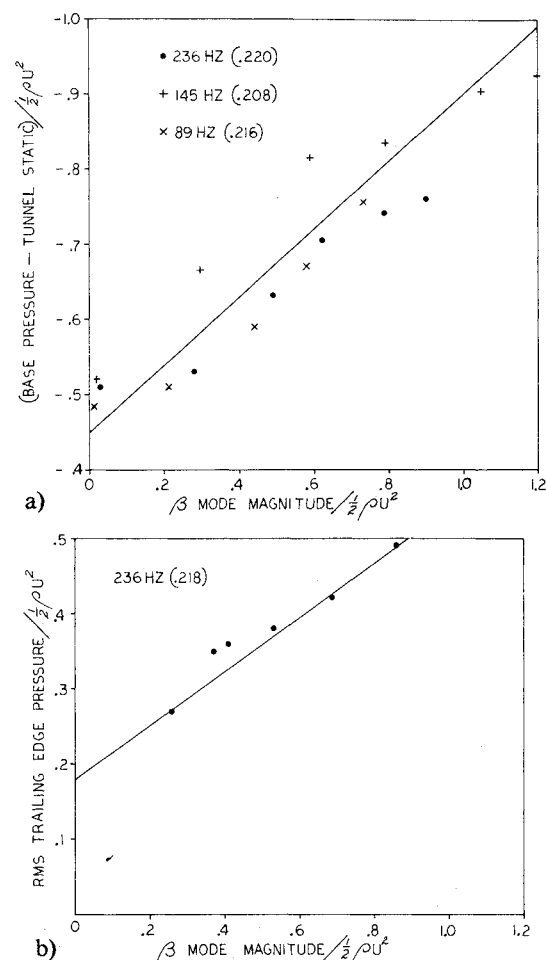


Fig. 4 The locked vortex shedding square base pressure coefficient plotted against the acoustic mode magnitude nondimensionalized by the dynamic head for three tunnel resonances at different Strouhal numbers.

base drag is due to the more intense vorticity in the von Karman street.

A definition of the proportionate increase of the correlated vortex shedding pressure ( $P_0$ ) above the residual value ( $P_0^*$ ) with no acoustic field ( $P_1$ ) present is used in Ref. 15 to represent the acoustic feedback gain in the self-excitation loop. It has a value of 2.0. Changing the unsteady vortex pressures in that definition to the steady base pressure coefficient  $C_p$  gives the equation below.

$$B = (\Delta C_p / C_p^*) / (\Delta P_1 / \frac{1}{2}\rho U^2)$$

Using curve 4A this parameter  $B$  has a value of 1.0. Thus the base pressure coefficient increases directly proportional to the applied acoustic field pressure nondimensionalized by the

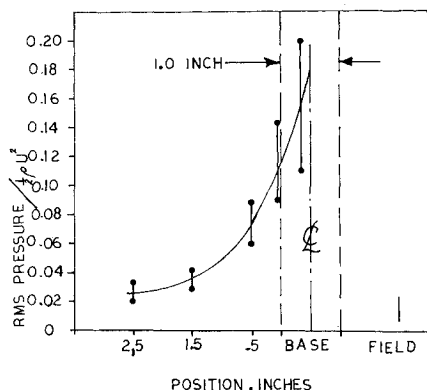


Fig. 5 The rms surface pressure distribution for natural uncorrelated vortex shedding from a square ended flat plate of 20 in. chord, obtained over a velocity range of 33 to 102 fps.

Table 2 Root mean square lift coefficients for natural vortex shedding

Trailing edge geometry	Pressure coefficient $\frac{1}{4}$ in. from trailing edge	Integrated trailing edge lift coefficient per base width per unit span $C_L$
Concave right angle	0.040	0.212
Square at end	0.150	0.375
Square $\frac{3}{4}$ in. from end	0.750	0.375
Convex right angle	0.100	0.450
Half round	0.110	0.550
Cylinder Ref. 19	...	0.40-0.80

dynamic head. The increase of the unsteady shed vorticity is the result of the increased acoustic velocities across the wake center line at the plate trailing edge associated with the three resonances.

Unsteady measurements of the drag were not made for the acoustically correlated case. However, unsteady pressure measurements were made along the chord and at the base for natural uncorrelated vortex shedding. Figure 5 shows that again the Kutta condition does not hold locally on the flat plate span for natural vortex shedding assuming that the pressure on the other side of the plate is  $180^\circ$  out of phase. The unsteady lift distribution rises toward the trailing edge and is confined to a region about half the distance of the acoustically correlated case.

These measurements were made using the signal from the various individually calibrated pressure taps on the surface and in the base. The magnitude was read from the Brüel and Kjaer amplifier on the slow rms meter setting. Associated with the mean rms value at a chordwise location there was a random amplitude fluctuation. The vertical bars indicate the extent of this unsteady lift coefficient variation from a number of tests at different tunnel velocities. In this case there was no significant nondimensional acoustic modal amplitude level as shown by the field line in the figure. The acoustic modal pressure in the trailing edge region would have been even lower, and therefore the pressures were not corrected for this component. Considering the range of the surface pressure values at a given location and the associated randomness this would be a doubtful exercise. In all cases the boundary layer was turbulent at the trailing edge ( $Re = 10^6$ ). The base Reynolds number was  $6 \times 10^4$  for the highest tunnel velocity. The curved line is drawn through the mean rms value and shows that the random unsteadiness increases toward the base centerline. The random variation at each position is attributed to the increase in the intensity of the spanwise unsteadiness that is expected to be more severe at the trailing edge. In fact

the magnitude of the random component is approximately proportional to the mean value of the unsteady lift.

Table 2 gives the local unsteady pressure coefficient  $P_0$  of natural vortex shedding and the integrated lift coefficient  $C_L$  for the various trailing edge shapes attached to the square trailing edge. The lift was calculated by doubling the measured rms pressure on one side and assuming that locally the shedding is  $180^\circ$  out of phase on the opposite side of the plate. Extrapolation of the measured pressure to the geometric trailing edge is possible for each geometry using the chordwise distribution for the square trailing edge; although the probable involvement of the convex shapes in the wake rolling-up region suggests caution. This objection is probably not so severe for the integrated lift. For all geometries, a linear distribution of 2.5 base lengths was used to approximate the actual distribution found for the square trailing edge. These values are in the second column of the table. At the bottom of the table, the uncorrelated lift values for a cylinder are given for comparison. These values were taken from Gerrard<sup>19</sup> for the same base Reynolds number.

The unsteady Kutta condition is next examined for the laminar boundary-layer instability. Tollmien-Schlichting waves on a 10C4 profile airfoil were discovered to be the cause of self-excitation of the  $\beta$  mode in the same test section of the low turbulence wind tunnel.<sup>16</sup> In the top part of Fig. 6 is shown the chordwise distribution of the surface pressure coefficient during self-excitation. The exponent of the exponential curve drawn through the data points was found from stability theory and the curve was scaled to pass through the point  $\frac{1}{2}$  in. from the trailing edge. The lower portion of the same figure shows the phase variation of a hot wire anemometer traversed along the chord and into the wake for a slightly different velocity and self-exciting frequency. The phase reference was the surface pressure  $1\frac{1}{2}$  in. from the trailing edge. The  $0.465 U_0$  phase curve on the airfoil portion corresponds to the instability wave speed measured at the extremes of the acoustic driving range. The  $0.9U$  phase curve corresponds to the convected Karman street speed which was found using measurements of the flow visualized wake from the flat plate. This convection speed for the rolled-up wake for the previous flat plate results was achieved within 2-3 base widths downstream.

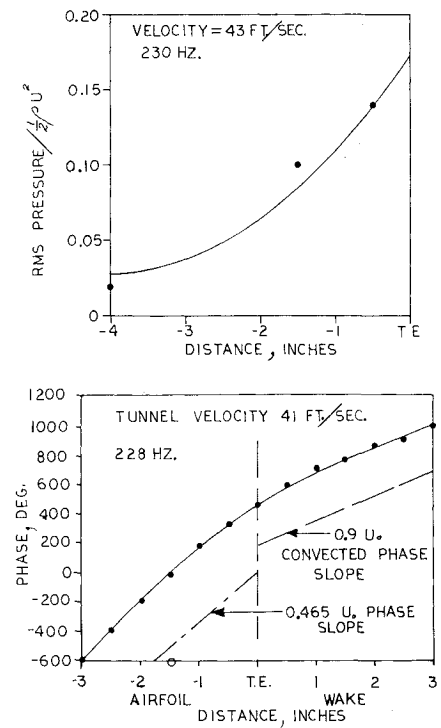


Fig. 6 The magnitude and phase of the boundary layer instability along the 10C4 airfoil during self-excitation of the  $\beta$  mode resonance.

The trailing edge loading coefficient shows surprising agreement for the two instability types. Since the wake in both cases exhibits the same convection velocities, it suggests that the shed vorticity from the laminar instability adjusts to form a wake closely related to the von Karman street of vortex shedding. Thus the resulting wake determines the trailing edge loading in both cases.

The purpose of testing the profile airfoil was to see whether the unsteady Kutta condition holds at high reduced frequencies ( $\lambda = \omega c/U$ ). Examining the wake perturbation with a hot wire anemometer confirmed that it was possible to drive the airfoil wake over the full velocity range of the tunnel with the loudspeakers. Consequently it was possible to investigate a wider range of frequency parameters than the flat plate. The lowest value 14 was achieved by driving the tunnel at its maximum speed and using the 145 Hz resonance. The amplitude of the perturbation was kept constant and not scaled with dynamic head. This would correspond, using Wood's<sup>18</sup> heaving analogy, to a constant amplitude of oscillation. The chordwise lift distribution shown in Fig. 7 was obtained using the same vector subtraction technique as described previously. This figure shows that the Kutta condition was not holding for these high reduced frequency parameters. The extrapolated surface pressure at the trailing edge is listed in Table 3. The driving acoustic amplitude used ensured that the boundary layer was always tripped turbulent during these tests.

For high  $\lambda$ , this pressure discrepancy is a small percent of the mode maximum acoustic perturbation. However, it is real. One can clearly see the microphone signal change its magnitude and phase when, without altering the applied acoustic energy, the wind tunnel is started from rest. In addition, Fig. 8 shows that this trailing edge pressure coefficient is directly related to the acoustic magnitude nondimensionalized by the dynamic head. There also appears to be a residual correlated trailing edge lift coefficient an order of magnitude lower than the vortex shedding value.

### III. Conclusions

Unsteady surface pressure data obtained near the trailing edge of a long flat plate and 10C4 airfoil have been presented. In all cases the real fluid effects of viscosity show a trailing edge loading indicating that the unsteady Kutta condition is not holding to the order of each instability type.

The magnitudes of the various fluid phenomena which form the hierarchy of disagreement are examined. Spanwise correlated vortex shedding is shown to have the greatest disagreement when locked at the Strouhal number of maximum response. The magnitude of the trailing edge loading has a Strouhal response like a damped-single-degree-of-freedom oscillator. The phase of the loading has a Strouhal response representative of a negatively damped oscillator that is characteristic of the instability mechanism. The increased base drag with increased acoustic mode as reported by Wood is shown to be associated with the increased shed vorticity in the Karman street. Natural vortex shedding is of next importance with the magnitude of local spanwise loading depending upon the trailing edge geometry.

Tables 1 and 2 present the integrated unsteady lift coefficients for the different trailing edge geometries for correlated and uncorrelated vortex shedding. These results are compared with the corresponding case for the circular cylin-

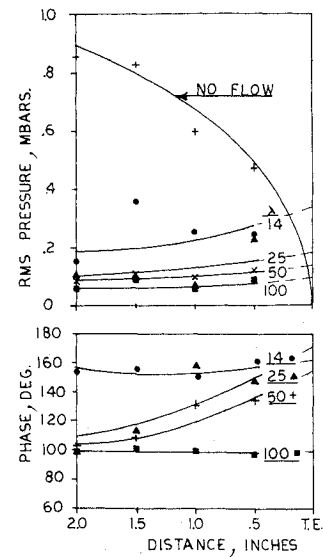


Fig. 7 The unsteady lift distribution on the 10C4 profile airfoil at different values of the reduced frequency parameter  $\lambda$  for a  $\beta$  mode magnitude of 137.9 dB = 1.60 mbars.

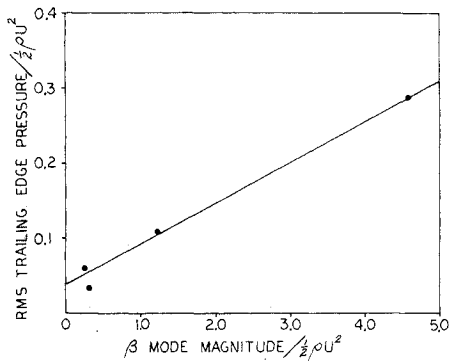


Fig. 8 Extrapolated trailing edge surface pressure coefficient plotted against the  $\beta$  mode magnitude nondimensionalized by the dynamic head.

der at the same base Reynolds number. The convex trailing edge geometries have the highest coefficient values in all cases indicative of more intense vortex shedding.

Pressure measurements of the acoustically coordinated Tollmien-Schlichting wavetrain on a 10C4 airfoil are reviewed. This laminar instability also violated the unsteady Kutta condition and the trailing edge loading distribution has been shown to agree with growth estimates from stability theory. The trailing edge lift coefficient for this acoustically coordinated instability is of the same order as residual correlated vortex shedding from a flat plate. This agreement is attributed to the formation region of a resulting Karman vortex street in both instances. The ratio of each boundary-layer thickness to the separated base region is probably of the same order for both airfoils.

The acoustic mode was used to simulate the heaving of an airfoil at high reduced frequency parameters. In this instance the boundary layer was turbulent. The trailing edge loading as

Table 3 The unsteady surface pressure distribution extrapolated to the trailing edge

Frequency parameter $\lambda = (\omega c/U)$	$\beta$ mode magnitude $1/2 \rho U^2$	Extrapolated pressure as percentage of mode magnitude	Extrapolated pressure $1/2 \rho U^2$	Phase degrees
14	0.28	21.3	0.059	162
25	0.31	11.1	0.034	170
50	1.23	8.8	0.108	154
100	4.57	6.3	0.288	100

a percentage of the constant amplitude of the acoustic mode decreased as the frequency parameter increased; while the phase of the surface pressure increased with frequency parameter. In addition the trailing edge pressure coefficient showed a similar linear relationship, above a residual value, with nondimensional acoustic amplitude as did vortex shedding.

Applying these results to practical situations suggests that for a turbulent boundary layer, the unsteady Kutta condition would not hold on a very local basis (on the order of the eddy correlation length scale). However, the integrated effect along the span would result in a nominally steady Kutta condition. The vortex shedding instability lift mechanism would be expected to affect the unsteady response of an airfoil due to the increase in the correlation coefficient and the increased shed vorticity if, associated with any unsteady perturbation, there were transverse velocities at the trailing edge at the Strouhal frequency. The trailing edge loading due to the laminar instability would rarely occur in practical situations since the freestream turbulence level, the noise level or an adverse chordwise pressure distribution would be sufficient to cause transition to a turbulent boundary layer.

## References

- 1 Kutta, W.M., *Auftriebskraefte in Stroemenden Fluessigkeiten, Illustrierte Aeronautische Mitteilungen*, July 1902, p. 133.
- 2 Taylor, G.I., "Note on the Connection Between the Lift on an Aerofoil in a Wind Tunnel and the Circulation Round It," Appendix to *Philosophical Transactions of the Royal Society at London, Series A*, 225, 1925; also printed as R&M 2725, Nov. 1949.
- 3 Preston, J.H., "The Calculation of Lift Taking Account of the Boundary Layer," R&M 2725, Aeronautical Research Council, London, Nov. 1949.
- 4 Gostello, J.P., "Viscosity Effects on the Two-Dimensional Flow Cascades," C.P. No. 872, Aeronautical Research Council, London.
- 5 Gredianus, J.H., Van de Vooren, A.I., and Bergh, H., "Experimental Determination of the Aerodynamic Coefficients of an Oscillating Wing in Incompressible, Two-Dimensional Flow," Parts I-IV, Repts. F.101-F.104, 1952, National Luchvaart-Laboratorium, Amsterdam, The Netherlands.
- 6 Theodorsen, T., "General Theory of Aerodynamic Instability and Mechanism of Flutter," Rept. 496, 1935, NACA.
- 7 Fujita, H. and Kovasznay, L.S.G., "Unsteady Responses of an Airfoil to Wake Cutting," *AIAA Journal*, Vol. 12, Sept. 1974, pp. 1216-1221.
- 8 Woolston, D.S. and Runyan, H.L., "Some Considerations on the Air Forces on a Wing Oscillating Between Two Walls for Subsonic Compressible Flow," *Journal of the Aeronautical Sciences*, Vol. 22, Jan. 1955, pp. 41-50.
- 9 Parker, R., "Resonance Effects in Wake Shedding from Parallel Plates: Calculations of Resonant Frequencies," *Journal of Sound and Vibration*, Vol. 5, 1967, pp. 332-343.
- 10 Whitehead, D.S., "Vibration and Sound Generation in a Cascade of Flat Plates in Subsonic Flow," R&M 3685, Aeronautical Research Council, London, Feb. 1970.
- 11 Smith, S.N., "Descrete Frequency Sound Generation in Turbo-Machines," R.M. 3709, Aeronautical Research Council, London.
- 12 Tanner, M., "A Method of Reducing the Base Drag of Wings with Blunt Trailing Edges," *The Aeronautical Quarterly*, Feb. 1972, Vol. 23, pp. 15-23.
- 13 Orszag, S.A. and Crow, S.C., "Instability of a Vortex Sheet Leaving a Semi-Infinite Plate," *Studies in Applied Mathematics*, Vol. XLIX, June 1970, pp.167-181.
- 14 Becher, D. and Pfizenmaier, E., "On the Kutta Condition at the Nozzle Discharge Edge in a Weakly Unsteady Flow," Deutsche Luft- und Raumfahrt, Rept. DLR FB 71-09 (1971), RAE Library Translation 1617, Sept. 1971.
- 15 Archibald, F.S., "The Self-Excitation of an Acoustic Resonance by Vortex Shedding," *Journal of Sound and Vibration*, Vol. 38, 1975, pp. 81-103.
- 16 Archibald, F.S., "The Laminar Boundary Layer Instability Excitation of an Acoustic Resonance," *Journal of Sound and Vibration*, Vol. 38, 1975, pp. 387-402.
- 17 Tanaka, H. and Takahara, S., "Study on Unsteady Aerodynamic Forces Acting on an Oscillating Cylinder," Proceedings of the 19th Japanese National Congress for Applied Mechanics, 1969 IV-9, pp. 162-166.
- 18 Wood, C.J., "The Effect of Lateral Vibrations on Vortex Shedding from Blunt-Based Aerofoils," *Journal of Sound and Vibration*, Vol. 14, 1971, pp. 91-102.
- 19 Gerrard, J.H., "An Experimental Investigation of the Oscillating Lift and Drag of a Circular Cylinder Shedding Turbulent Vortices," *Journal of Fluid Mechanics*, Vol. 11, 1961, pp. 244-256.